Available online at www.sciencedirect.com
ScienceDirect
Ceramics International 37 (2011) 2609–2613
CERAMICS INTERNATIONAL
www.elsevier.com/locate/ceramint

Synthesis and thermoelectric performance of Ta doped $Sr_{0.9}La_{0.1}TiO_3$ ceramics

H.C. Wang [a,*], C.L. Wang [a], W.B. Su [a], J. Liu [a], H. Peng [a], Y. Sun [a,b], J.L. Zhang [a], M.L. Zhao [a], J.C. Li [a], N. Yin [a], L.M. Mei [a]

[a] School of Physics, State Key Laboratory of Crystal Materials, Shandong University, No. 27 Shanda Nan Road, Jinan 250100, PR China
[b] Department of Physics, Changji University, Changji 831100, PR China

Received 10 January 2011; received in revised form 3 April 2011; accepted 5 April 2011
Available online 14 April 2011

Abstract

Ceramics samples of $Sr_{0.9}La_{0.1}Ti_{1-x}Ta_xO_3$ have been synthesized by conventional solid-state reaction method. X-ray powder diffraction characterization indicates that all samples are of single phase with cubic symmetry. The high-temperature electrical resistivity decreases with the increasing of tantalum content except for $x = 0.05$ sample. Negative Seebeck coefficients have been obtained for all samples, which means conduction mechanism being n-type. The absolute Seebeck coefficient decreases with the increase of tantalum concentration. The power factor decreases with increasing of tantalum substitution. Small amount tantalum doping can reduce the thermal conductivity. The lowest thermal conductivity obtained is 2.9 W/mK for $x = 0.03$ at 1074 K. The highest thermoelectric figure of merit still observes in $Sr_{0.9}La_{0.1}TiO_3$, reaches 0.29 at 1046 K, which is a relatively higher value in n-type oxide thermoelectric materials.

PACS : 65.20.+W; 72.15.Jf; 72.20.pa

Keywords: C. Electrical properties; C. Thermal conductivity; D. Transition metal oxides

1. Introduction

Oxide thermoelectric materials have drawn much attention in recent years because of their high thermal stability, lower cost and no toxicity. Both high electrical power factor and low thermal conductivity have been found in p-type oxide materials such as $NaCo_2O_4$ and $Ca_3Co_4O_9$ materials [1–5]. On the other hand, n-type oxide thermoelectric materials are inevitably required as a counter-partner of the p-type oxide materials for build-up thermoelectric modules. It has been reported that n-type lanthanum-doped $SrTiO_3$ single crystal exhibits high power factor, which is comparable with that of Bi–Te alloy at room temperature [6]. Rare earth doped $SrTiO_3$ ceramics have been prepared and their thermoelectric properties have been studied [7]. The most appropriate amount of lanthanum has been estimated as about 10 mol% by considering the contributions of electronic thermal conductivity. The figure of merit can be enhanced, if its thermal conductivity could be reduced. Fortunately, a relatively low thermal conductivity about 3W/mK at 1000 K has been achieved in niobium-doped $SrTiO_3$ epitaxial film [8]. The figure of merit for $SrTi_{0.8}Nb_{0.2}O_3$ has reached 0.37 at 1000 K, which was the largest value among n-type oxide semiconductors ever reported then. Normally the thermal conductivity is associated to the ion mass difference between dopant and matrix [9]. In this sense, tantalum doping may reduce the lattice thermal conductivity in comparison with niobium doping, hence improving the figure of merit. To confirm this issue, tantalum doped $Sr_{0.9}La_{0.1}TiO_3$ ceramic samples have been prepared in this work, and their thermoelectric properties have been investigated.

2. Experimental

Ceramic samples of $Sr_{0.9}La_{0.1}Ti_{1-x}Ta_xO_3$ with $x = 0.00$, 0.01, 0.03, 0.05 have been prepared by conventional solid state reaction technique. The starting materials are La_2O_3 with purity of 99.99%, $SrCO_3$ of 99%, TiO_2 of 99.8%, and Ta_2O_5 of 99.5%, respectively. The raw materials are weighted in stoichiometric

* Corresponding author. Tel.: +86 531 88377035; fax: +86 531 88377031.
E-mail address: wanghongchao@mail.sdu.edu.cn (H.C. Wang).

0272-8842/$36.00
doi:10.1016/j.ceramint.2011.04.004

proportions, and mixed by ball-milling in ethanol with zirconia balls for 12 h. After the wet mixtures have been dried, they are pressed into pellets, and calcined at 1350 °C for 6 h in ambient. The pellets are smashed and ball-milled for 12 h. Then the powder is repressed into pellets. These pellets are sintered at 1460 °C for 4 h in the presence of argon gas with 5 mol% hydrogen. The sintered discs are cut into rectangular columns with geometry 20 mm × 1.8 mm × 1.8 mm for measurements.

Crystal structure is characterized by X-ray powder diffraction with Cu Kα radiation (λ = 0.154056 nm) utilizing a Bruker AXS D8 advance diffractometer. The surface morphology is obtained on a S4800 scanning electronic microscope (SEM). Electrical resistivity and Seebeck coefficient are measured simultaneously in the temperature range of 300–1100 K using a ULVAC ZEM-3 equipment in Helium atmosphere. Thermal diffusivity and specific capacity are measured by a laser flash apparatus (Netzsch LFA 427) and a different thermal analyzer (Netzsch STA 449C), respectively. The thermal conductivity is calculated from the thermal diffusivity, the specific heat capacity, and the sample density. The figure of merit is calculated from above measured the electrical resistivity and the thermal conductivity.

3. Results and discussion

X-ray powder diffraction patterns are presented in Fig. 1. It can be seen that the XRD patterns of the ceramics with $x = 0.01$, 0.03, 0.05 are the same as that of $Sr_{0.9}La_{0.1}TiO_3$ sample, indicative of tantalum element being doped into the lattice of $Sr_{0.9}La_{0.1}TiO_3$ and formed a single phase compound. Referred to the PDF card of No. 35-0734, all samples are of single phase in cubic symmetry. The major diffraction peaks can be indexed with the cubic perovskite structure belonging to the Pm3m space group. All the peaks in Fig. 1 slightly shift to small angle position with the increase of tantalum content, implies that the lattice is expanded by the doped tantalum. The lattice constants and lattice volumes are calculated and presented in Fig. 2. The lattice constant of $Sr_{0.9}La_{0.1}TiO_3$ is 3.9067 Å, which is in agreement with that of early report [7]. With the increase of

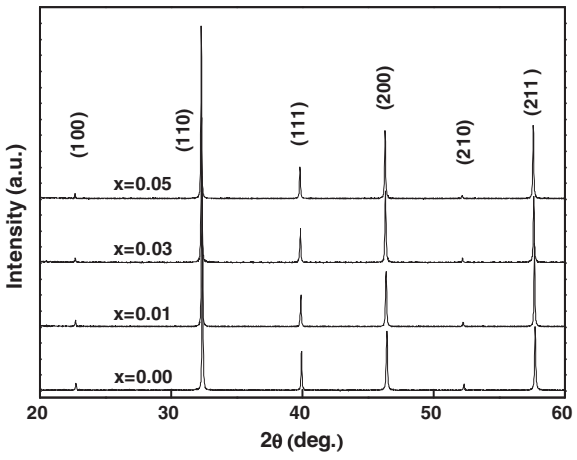

Fig. 1. X-ray powder diffraction patterns of $Sr_{0.9}La_{0.1}Ti_{1-x}Ta_xO_3$ with $x = 0.00$, 0.01, 0.03, 0.05.

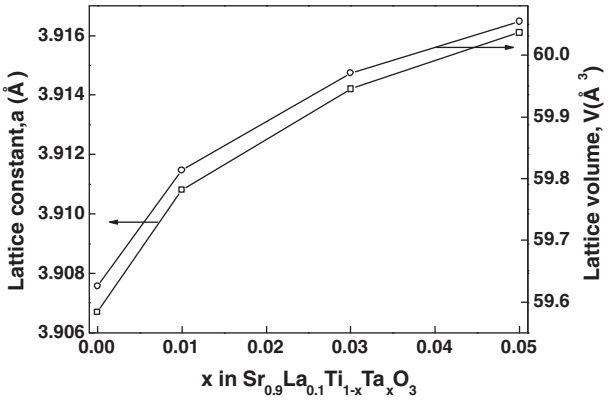

Fig. 2. The lattice constants and lattice volume of $Sr_{0.9}La_{0.1}Ti_{1-x}Ta_xO_3$ for different tantalum content.

tantalum content, the lattice constants and lattice volumes increase. The formation of Ti^{3+} can be considered by Ta doping, using the Kroger–Vink notation as $Sr_{0.9}La_{0.1}(Ta_x^{5+}Ti_{1-x-y}^{4+}Ti_y^{3+})O_3$. Although the ionic radius for Ti^{4+} and Ta^{5+} are same of 0.68 Å, the content of Ti^{3+} may increase with increase of Ta^{5+}, and the ionic radius of Ti^{3+} (0.76 Å) is larger. The theoretical density of all samples is calculated from the lattice constants. The relative density, which is the measured density over the theoretical density, are 89.2%, 87.6%, 85.9%, 87.8% for $x = 0.00$, 0.01, 0.03, 0.05, respectively. The fluctuation of density is not much large. Therefore, we may not consider the effect of porous on the thermoelectric properties described in the later.Fig. 3a–d is scanning electronic microscope (SEM) images of surface microstructures for $Sr_{0.9}La_{0.1}Ti_{1-x}Ta_xO_3$ ceramics. These images exhibit the typical morphology of sintered ceramics obtained by the solid state reaction. We can see from these SEM images that the grain size decreases with the increase of tantalum. The density was measured by the Archimedes' method, which are 4.7024 g/cm^3, 4.6850 g/cm^3, 4.6195 g/cm^3, 4.5819 g/cm^3, 4.7394 g/cm^3 for $x = 0.00$, 0.01, 0.03, 0.05, respectively.Temperature dependence of the electrical resistivity of $Sr_{0.9}La_{0.1}Ti_{1-x}Ta_xO_3$ is shown in Fig. 4. The electrical resistivity for $Sr_{0.9}La_{0.1}TiO_3$ ceramic is lower than that in an early report [7], especially in high temperature range. The electrical resistivity decreases with the increasing of temperature when temperature is lower than 500 K, but increases with further increasing of the temperature. Their semiconductivity behavior in low temperature is in accordance with the reports of polycrystalline sample [7]. As similar behavior has not been observed in single crystal samples [6], the semiconductivity behavior can be due to the scattering of grain boundaries [7]. With small mount of tantalum substitution, the electrical resistivity is not effectively changed, see curves for $x = 0.01$ and 0.03 in Fig. 4, though there is a small reduction of the electrical resistivity in high temperature end. The decrease of resistivity can be explained by the Kroger–Vink equation. The Kroger–Vink reaction is $2Ta_2O_5 \rightarrow 4Ta_{Ti}^{+} + 10O_o^{\times} + V_{Ti}^{4-}$, where Ta_{Ti}^{+} represent donor doping center. Therefore, Ta doping can increase the concentration of carriers, and decrease the electrical resistivity. With the further increase of tantalum content, see curve of

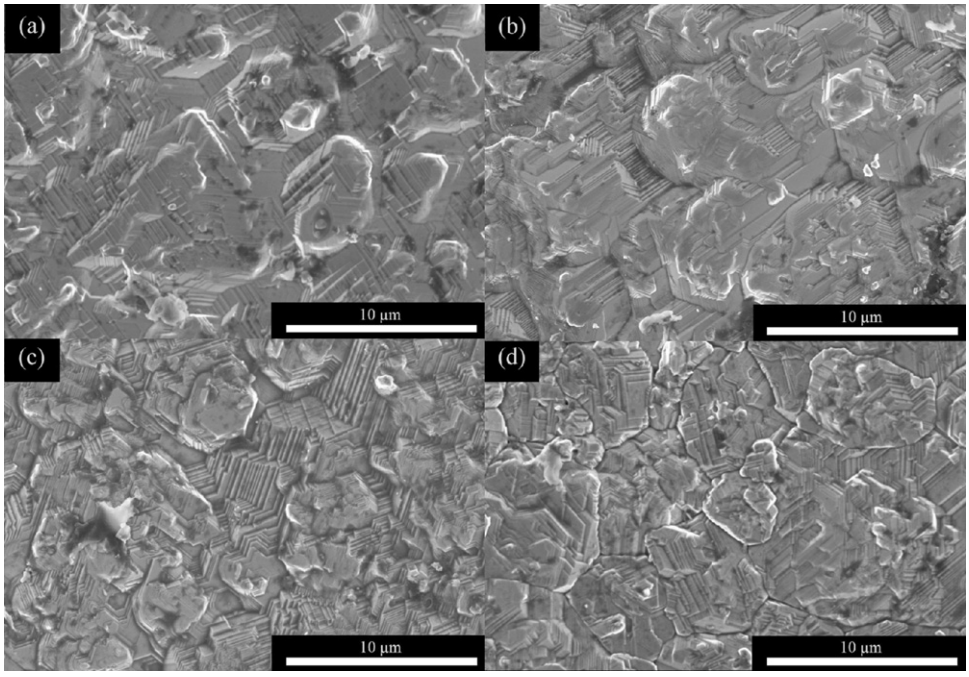

Fig. 3. SEM images of surface section for $Sr_{0.9}La_{0.1}Ti_{1-x}Ta_xO_3$ ceramics for $x = 0.00$, 0.01, 0.03, and 0.05 in (a), (b), (c), and (d), respectively.

$x = 0.05$, the electrical resistivity is much increased. This behavior is similar with that of the niobium and tantalum doped $CaMnO_3$ system [10]. Though tantalum doping can introduce more carriers, it also introduces scattering centers, especially at high doping level. With the increase of tantalum content, this strong scattering may become dominating factor for electron conduction, resulting in increase of electrical resistivity. By fitting the resistivity to a power law relationship $(\rho(T) - \rho_0) \propto T^{\gamma}$ [11] in high temperatures range, we obtained that $\gamma = 2.5$, 2.6, 2.8, 2.9 for $x = 0.00$, 0.01, 0.03, 0.05, respectively. The electrical resistivity increases with temperature in a much quicker manner in high temperature range. The minimum value of electrical resistivity shifts to higher temperature as more tantalum is doped, and the lowest value of electrical resistivity is 1.4 mΩ cm for $x = 0.01$ of tantalum contents.

The temperature dependence of the Seebeck coefficient is shown in Fig. 5. The values of Seebeck coefficient are all negative, indicating of n-type electrical conduction. With the increasing of tantalum content, the absolute value of Seebeck coefficient decreases. This could be attributed to the increase of carrier concentration as more tantalum doped. In addition, we notice that the absolute Seebeck coefficient decreases with increasing of the lattice constants as shown in Fig. 2. This behavior is similar to what is observed in samples of Lanthanum doped $SrTiO_3$ single crystalline [12]. The Seebeck coefficient is nearly a linear function of temperature from 300 K to 1100 K. The linear relationship of Seebeck coefficients with temperature implies a metallic behavior of the electron conduction, and can be expressed as [11,13,14].

$$S \sim \pi^2 k_B^2 T / e E_F \quad (1)$$

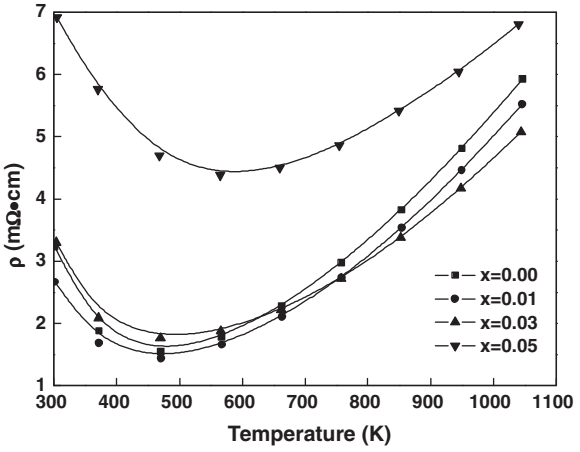

Fig. 4. Temperature dependence of electrical resistivity of $Sr_{0.9}La_{0.1}Ti_{1-x}Ta_xO_3$ ceramics.

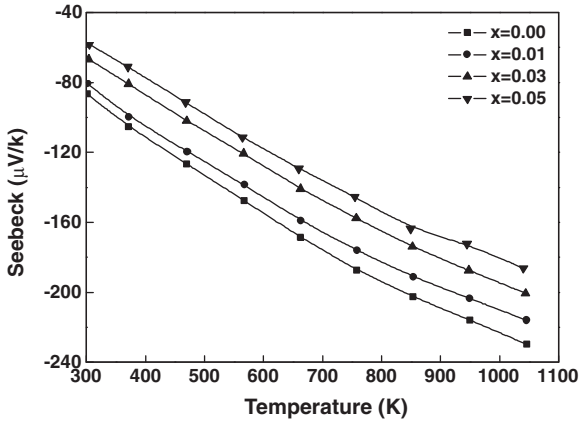

Fig. 5. Temperature dependence of the Seebeck coefficients of $Sr_{0.9}La_{0.1}Ti_{1-x}Ta_xO_3$ ceramics.

where E_F is the Fermi level, and k_B and e are Boltzmann constant and electron charge, respectively. This formula indicates that the Seebeck coefficient is inversely proportional to Fermi level E_F. By fitting the experimental data in Fig. 5 with Eq. (1) using the least square method, we obtain the values of the Fermi level. They are 0.348 eV, 0.367 eV, 0.372 eV, 0.378 eV for $x = 0.00$, 0.01, 0.03, 0.05, respectively. This means that the tantalum doping increases the Fermi level in $Sr_{0.9}La_{0.1}TiO_3$. When Ta^{5+} substitutes Ti^{4+} in $Sr_{0.9}La_{0.1}TiO_3$, the Ta^{5+} is expected to behave as donor ion. This leads to the increase of carrier concentration, and shift of the occupied energy level structure to higher binding energy. Therefore, the Fermi level will increase with the increasing of tantalum content.

The temperature dependence of the power factors are presented in Fig. 6. The power factors for $x = 0.00$, 0.01, 0.03 increase with the increasing temperature, reach a maximum, and then slightly decrease with further increase of temperature. The power factor of $x = 0.05$ still increases with increasing temperature. The un-doped sample still maintains the highest values of power factor. The power factor decreases with increasing of tantalum content. The maximum of power factor for ceramic samples decreases from 1247 $\mu W/K^2m$ for $x = 0.00$ to 509 $\mu W/K^2m$ for $x = 0.05$. The reduction of the power factor with tantalum substitution is the result of the reduction of absolute value of the Seebeck coefficient.

Temperature dependence of total thermal conductivity is shown in Fig. 7a. The electronic thermal conductivity is shown in Fig. 7b, which is calculated from Wiedemann–Franz law $\kappa_e = LT/\rho$, with Lorentz number $L = 2.44 \times 10^{-8}\ V^2\ K^{-2}$ for free electrons. The thermal conductivity at room-temperature is about 6.1 W/mK for un-doped sample. This value is more or lees the same as that from Muta et al. [15]. The thermal conductivity decreases monotonically with increasing of temperature. The tantalum substitution does reduce the thermal conductivity. Doping contents of $x = 0.03$ has the optimized effect for reducing the thermal conductivity. The value of the thermal conductivity for $x = 0.03$ decreases from 5.5 W/mK at 328 K to 2.9 W/mK at 1074 K, which is the lowest thermal conductivity in our samples. The lowest value of the thermal

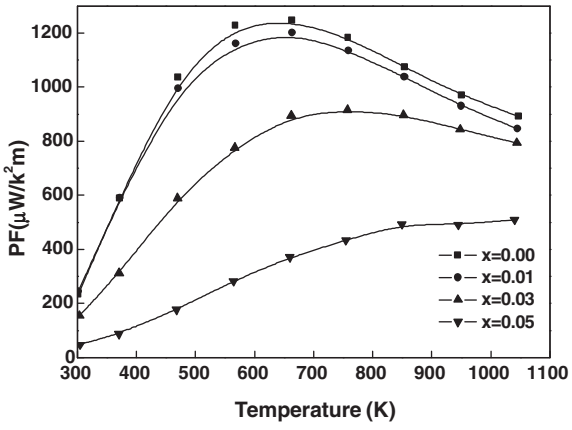

Fig. 6. Temperature dependence of the power factor of $Sr_{0.9}La_{0.1}Ti_{1-x}Ta_xO_3$ ceramics.

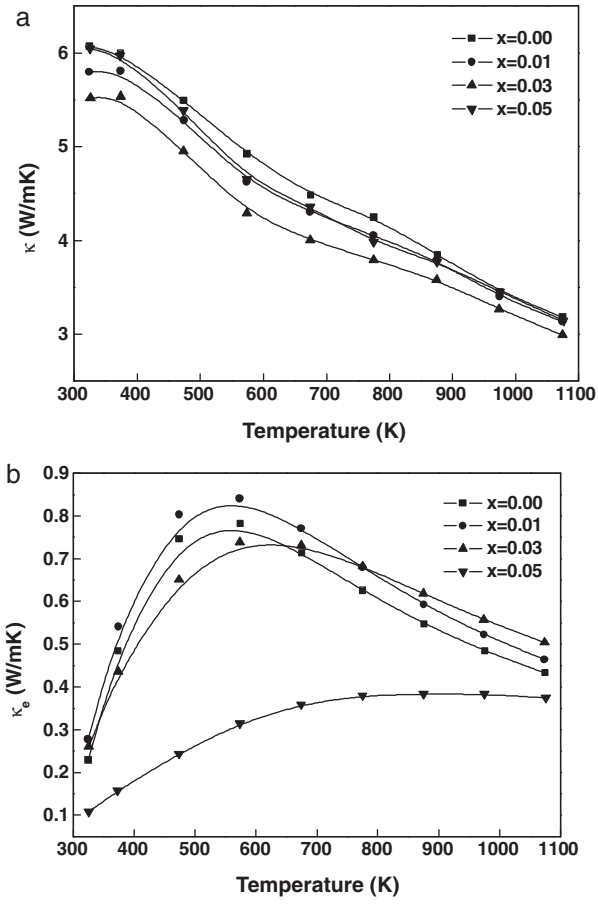

Fig. 7. Temperature dependence of the thermal conductivity (a) and electronic thermal conductivity (b) of $Sr_{0.9}La_{0.1}Ti_{1-x}Ta_xO_3$ ceramics.

conductivity in sample of $x = 0.03$ is resulted from the reduction of the lattice thermal conductivity. Since the thermal conductivity can be expressed by the sum of lattice contribution (κ_L) and electronic contribution (κ_e) as $\kappa = \kappa_L + \kappa_e$. As can be seen in Fig. 6b, the electronic thermal conductivity makes a small contribution to the total thermal conductivity, In room temperature, we estimate the electronic contribution to the total thermal conductivity in $Sr_{0.9}La_{0.1}Ti_{1-x}Ta_xO_3$ ceramics is about 3.8%, 4.8%, 4.7%, 1.8%, for $x = 0.00$, 0.01, 0.03, 0.05, respectively. This means that the total thermal conductivity comes mainly from the lattice vibrations. Therefore, the decrease of thermal conductivity mainly comes from the decrease of lattice thermal conductivity by doping tantalum.

Temperature dependence of dimensionless figure of merit ZT is shown in Fig. 8 for different tantalum substitutions. We can see that ZT value for all samples increases with increasing temperature monotonically. The ZT value for $x = 0.01$ sample nearly same with that for $x = 0.00$, except for a slightly reduction at the high temperatures. For $x = 0.03$ and 0.05 samples, the reduction of ZT values with tantalum doping is quite obviously. That means tantalum doping in $Sr_{0.9}La_{0.1}Ti_1O_3$ contents do not have positive effect from point view of ZT values. Although the thermal conductivity is reduced by introducing of tantalum, the much more reduction of the power factor finally reduces the ZT values. Therefore, $Sr_{0.9}La_{0.1}TiO_3$

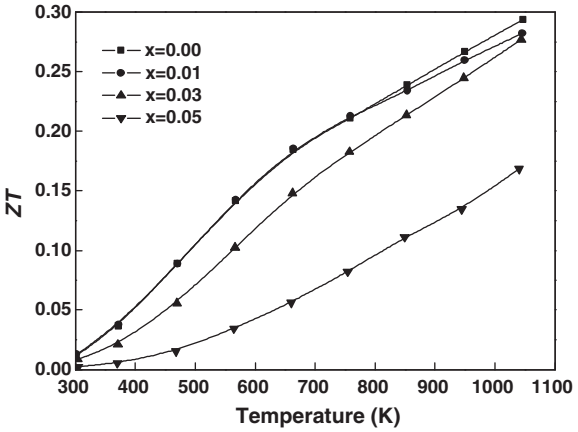

Fig. 8. Temperature dependence of the figure of merit of $Sr_{0.9}La_{0.1}Ti_{1-x}Ta_xO_3$ ceramics.

ceramic still maintains the highest value of 0.29 at 1046 K in our studies.

4. Summary

We prepared the $Sr_{0.9}La_{0.1}Ti_{1-x}Ta_xO_3$ with $x = 0.00$, 0.01, 0.03, 0.05 ceramics. All the samples are of cubic perovskite symmetry with the lattice parameter increases with increasing tantalum content. The effects of tantalum substitution for titanium on the thermoelectric properties are investigated at temperatures from 300 K to 1100 K. We find that the absolute Seebeck coefficient obviously decreases gradually with the tantalum substitution. Therefore, the power factor is lower than that of un-doped sample. The thermal conductivity is decreased by tantalum substitution, and this behavior confirms our previous idea. However, the thermoelectric performance has not been improved by the tantalum doping in our work.

Acknowledgements

The work is financially supported by National Basic Research Program of China of 2007CB607504, Natural Science Fund of China under grant nos. 50902086 and 50572052, Shandong Province Natural Science Foundation under grant no.ZR2009AQ003, Graduate Independent Innovation Foundation of Shandong University under grant No. yzc09076, Academic Creative Scholarship Foundation for Doctors of Ministry of Education, and Fostering Foundation for Excellent PhD of Shandong University.

References

[1] I. Terasaki, Y. Sasago, K. Uchinokura, Large thermoelectric power in $NaCo_2O_4$ single crystals, Phys. Rev. B 56 (1997) R12685–R12687.
[2] Y.F. Zhang, J.X. Zhang, Q.M. Lu, Synthesis of highly textured $Ca_3Co_4O_9$ ceramics by spark plasma sintering, Ceram. Int. 33 (2007) 1305–1308.
[3] Y. Song, Q. Sun, L.R. Zhao, F.P. Wang, Z.H. Jiang, Synthesis and thermoelectric power factor of $(Ca_{0.95}Bi_{0.05})_3Co_4O_9$/Ag composites, Mater. Chem. Phys. 113 (2009) 645–649.
[4] Y.-H. Lin, J. Lan, Z. Shen, Y. Liu, C.-W. Nan, J.-F. Li, High-temperature electrical transport behaviors in textured $Ca_3Co_4O_9$-based polycrystalline ceramics, Appl. Phys. Lett. 94 (2009) 072107.
[5] H.Q. Liu, X.B. Zhao, T.J. Zhu, Thermoelectric properties of Gd, Y co-doped $Ca_3Co_4O_{9+\delta}$, Curr. Appl. Phys. 9 (2009) 409–413.
[6] T. Okuda, K. Nakanishi, S. Miyasaka, Y. Tokura, Large thermoelectric response of metallic perovskites: $Sr_{1-x}La_xTiO_3$ ($0 \leq x \leq 0.1$), Phys. Rev. B 63 (2001) 113104.
[7] H. Muta, K. Kurosaki, S. Ymanaka, Thermoelectric properties of rare earth doped $SrTiO_3$, J. Alloys Compd. 350 (2003) 292–295.
[8] S. Ohta, T. Nomura, H. Ohta, K. Koumoto, Large thermoelectric performance of heavily Nb-doped $SrTiO_3$ epitaxial film at high temperature, Appl. Phys. Lett. 87 (2005) 092108.
[9] B. Abeles, Lattice thermal conductivity of disordered semiconductor alloys at high temperatures, Phys. Rev. 131 (1963) 1906–1911.
[10] G.J. Xu, R. Funahashi, Q. Pu, B. Liu, R. Tao, G.S. Wang, Z.J. Ding, High-temperature transport properties of Nb and Ta substituted $CaMnO_3$ system, Solid State Ionics 171 (2004) 147–151.
[11] D. Li, X.Y. Qin, J. Zhang, L. Wang, H.J. Li, Enhanced thermoelectric properties of bismuth intercalated compounds Bi_xTiS_2, Solid State Commun. 135 (2005) 237–240.
[12] H. Muta, K. Kurosaki, S. Ymanaka, Thermoelectric properties of reduced and La-doped single-crystalline $SrTiO_3$, J. Alloys Compd. 392 (2005) 306–309.
[13] H.C. Wang, C.L. Wang, W.B. Su, J. Liu, H. Peng, J.L. Zhang, M.L. Zhao, J.C. Li, N. Yin, L.M. Mei, Substitution effect on the thermoelectric properties of reduced Nb-doped $Sr_{0.95}La_{0.05}TiO_3$ ceramics, J. Alloys Compd. 486 (2009) 693–696.
[14] H.C. Wang, C.L. Wang, W.B. Su, J. Liu, Y. Zhao, H. Peng, J.L. Zhang, M.L. Zhao, J.C. Li, N. Yin, L.M. Mei, Enhancement of thermoelectric figure of merit by doping Dy in $La_{0.1}Sr_{0.9}TiO_3$ ceramic, Mater. Res. Bull. 45 (2010) 809–812.
[15] H. Muta, K. Kurosaki, S. Yamanaka, Thermoelectric properties of doped $BaTiO_3$–$SrTiO_3$ solid solution, J. Alloys Compd. 368 (2004) 22–24.